Annals of Nuclear Medicine Vol. 17, No. 6, 511–515, 2003

Imaging of adenosine A_1 receptors in the human brain by positron emission tomography with [^{11}C]MPDX

Nobuyoshi FUKUMITSU,*,** Kenji ISHII,* Yuichi KIMURA,* Keiichi ODA,*
Toru SASAKI,* Yutaka MORI** and Kiichi ISHIWATA*

*Positron Medical Center, Tokyo Metropolitan Institute of Gerontology
**Department of Radiology, Jikei University School of Medicine

We report the first clinical PET study using [1-methyl-^{11}C]8-dicyclopropylmethyl-1-methyl-3-propylxanthine ([^{11}C]MPDX) for imaging adenosine A_1 receptors in the human brain. The binding of [^{11}C]MPDX evaluated quantitatively as the distribution volume by a graphical analysis was high in the striatum and thalamus, and low in the cerebellum. The distribution pattern of [^{11}C]MPDX was coincident with that of adenosine A_1 receptors *in vitro* reported previously, and was different from those of blood flow and [^{18}F]FDG. The [^{11}C]MPDX PET has the potential for mapping adenosine A_1 receptors in the human brain.

Key words: [^{11}C]MPDX, adenosine A_1 receptor, positron emission tomography

INTRODUCTION

ADENOSINE is present in large amounts in the mammalian brain and plays a role as an endogenous modulator of synaptic functions in the central nervous system. The effects are mediated by two major subtypes of receptors: A_1 and A_2 receptors. The adenosine A_1 receptors exhibit a higher affinity for adenosine and inhibit adenylyl cyclase. The A_2 receptors exhibit a lower affinity for adenosine and stimulate adenylyl cyclase, and are further divided into A_{2A} and A_{2B} subtypes. It is now known that A_1 receptors are G protein-linked and can act through effectors other than adenylyl cyclase, including potassium channels, calcium channels, phospholipase A_2 and C, and guanylyl cyclase.[1] For the purpose of mapping of adenosine A_1 and A_{2A} receptors in the brain by positron emission tomography (PET), we synthesized and characterized several radioligands (see references in reviews).[2,3] Among them, [1-methyl-^{11}C]8-dicyclopropylmethyl-1-methyl-3-propylxanthine ([^{11}C]MPDX) was the PET ligand of choice for mapping adenosine A_1 receptors.[4–7] In a preclinical study including the imaging of adenosine A_1 receptors of the monkey brain by PET, we proved [^{11}C]MPDX to be a suitable PET radioligand for human studies.[6] This is the first application of [^{11}C]MPDX for mapping adenosine A_1 receptors in the human brain by PET. The distribution of the adenosine A_1 receptors was compared with the images of cerebral blood flow and glucose metabolism in the same individual.

Received January 14, 2003, revision accepted May 16, 2003.
For reprint contact: Nobuyoshi Fukumitsu, M.D., Department of Radiology, Jikei University School of Medicine, 3–25–8, Nishi-shinbashi, Minato-ku, Tokyo 105–8461, JAPAN.
E-mail: GZL13162@nifty.ne.jp

MATERIALS AND METHODS

A 51-year-old male normal volunteer who had no neurological findings and no abnormality on brain MRI underwent PET scans with [^{15}O]water, [^{11}C]MPDX, and [^{18}F]FDG. PET measurement was performed with SET-2400W (Shimadzu Co., Kyoto, Japan). The study protocol was approved by the Institutional Ethical Committee, and written informed consent was obtained from the subject.

After transmission scan with a rotating [^{68}Ga]/[^{68}Ge] line source to correct for the photon attenuation using the attenuation map, [^{15}O]water (150 MBq) was injected intravenously for a period of 10 sec. Then PET scan was performed for 120 sec in a 3D static mode. Ten min later, [^{11}C]MPDX[4] (610 MBq/14 nmol) was injected intravenously for a period of 10 sec. PET scan was performed for 90 min in a 2D dynamic mode (10 sec × 6 frames, 30

sec × 3 frames, 60 sec × 5 frames, 150 sec × 5 frames, 300 sec × 14 frames). The tomographic images were reconstructed using a filtered backprojection method, and Butterworth filter (cutoff frequency 1.25 cycle/cm and order of 2). The data were collected in a 128 × 128 × 25 slices × 33 matrix. The voxel size was 2 × 2 × 6.25 mm. Arterial blood was taken at 10, 20, 30, 40, 50, 60 70, 80, 90, 100, 110, 120, 135, and 150 sec, and 3, 5, 7, 10, 15, 20, 30, 40, 50, 60, 70, 80, and 90 min, and the plasma radioactivity level was measured. The unchanged form of [^{11}C]MPDX in the plasma sampled at 3, 10, 20, 30, 40, and 60 min was analyzed by high-performance liquid chromatography as described previously.[4]

On another day, [^{18}F]FDG (130 MBq) was injected into the same subject, and the 6-min PET scan with a 3D static mode was started 45 min after the injection.

PET images were registered and resliced to MRI by UNIX workstations (Silicon Graphics Inc., Mountain View, CA, USA) using the Dr. View image analysis software system (Asahi Kasei Joho System, Tokyo, Japan).[8] Regions of interest (ROIs) were placed on the frontal, medial frontal, temporal, medial temporal, parietal, and occipital cortices, striatum, thalamus, and cerebellum based on MRI. Time-activity curves (TACs) in each region of the brain and in plasma were calculated. Using the TACs in the tissues and the metabolite-corrected TAC in plasma, the distribution volume (DV) for [^{11}C]MPDX was evaluated using a graphical analysis by Logan et al.[9]

RESULTS

Figure 1 shows the PET images of [^{11}C]MPDX, [^{15}O]water, and [^{18}F]FDG. [^{11}C]MPDX was widely distributed with different concentrations in the brain. The three images were similar, but a few differences were found. Uptake of [^{11}C]MPDX or [^{18}F]FDG was prominent in the striatum compared with that of [^{15}O]water, while the latter was relatively higher in the thalamus and cerebellum than the former.

Figure 2 shows the TACs in the brain tissues and in plasma after injection of [^{11}C]MPDX. [^{11}C]MPDX was taken at high levels in all regions investigated, and the levels were decreased for first 15 min after injection. The radioactivity level in plasma rapidly decreased. Percentages of unchanged forms of [^{11}C]MPDX were 99.4% at 3 min, 87.0% at 10 min, 75.3% at 20 min, 73.5% at 30 min, 71.1% at 40 min, and 70.7% at 60 min.

The DV for [^{11}C]MPDX was large in the striatum (1.34) and thalamus (1.30), medium in the occipital (1.21), parietal (1.19), temporal (1.19), frontal (1.16), medial frontal (1.13) and medial temporal cortices (1.09), and small in the cerebellum (0.95).

Figure 3 shows the relative distribution of the three tracers investigated in the brain. The DV of [^{11}C]MPDX and uptake of [^{15}O]water or [^{18}F]FDG in each of the brain regions were normalized so that the respective value in the cerebellum became 1. The distribution patterns of the three tracers differed from each other. The binding of [^{11}C]MPDX was relatively high in the striatum and thalamus and lowest in the cerebellum, while the blood flow in the cerebellum was relatively high among the regions investigated.

DISCUSSION

Recently we performed mapping of adenosine A_1 receptors in the brain of cats and monkeys by the PET with [^{11}C]MPDX.[5,6] The present first clinical study showed that [^{11}C]MPDX has potential as a PET ligand for mapping of adenosine A_1 receptors in human studies. [^{11}C]MPDX was taken up well by the brain, but the levels of radioactivity in all regions investigated deceased relatively faster than those in the brain of cats and monkeys.

The brain kinetics of [^{11}C]MPDX is affected by several factors *in vivo*. The fast clearance pattern of [^{11}C]MPDX is mainly due to the affinity of [^{11}C]MPDX for adenosine A_1 receptors. In general, Ki = 4.2 of [^{11}C]MPDX for the adenosine A_1 receptors[4] was relatively weak compared with those of other radioligands for neuroreceptors. In the present study, we did not evaluate the specific binding of [^{11}C]MPDX, while blocking studies were performed previously in experimental animals. A PET study showed that the specific DV of [^{11}C]MPDX was 53% of the total DV in the cerebral cortex of cats.[5] An *ex vivo* autoradiographic study showed that the specific binding of [^{11}C]MPDX was 60% in the rat brain 15 min after the tracer injection.[7] The specific binding of [^{11}C]MPDX was 60–70% in the mouse brain and rabbit brain (unpublished data). Because of faster clearance patterns in the human brain than in animal brains, the ratio of specific binding in humans may be lower than those observed in experimental animals. It is known that the injected doses also influence the kinetics of the receptor radioligands. The maximal concentration of MPDX in the brain, which was calculated from the uptake level (Bq/m*l*) and the specific activity (44 MBq/nmol) of [^{11}C]MPDX, was approximately 1 pmol/m*l* immediately after the injection. This value corresponds to at most 10% of the density of the adenosine A_1 receptors which was estimated at most 10 fmol/mg gray matter by *in vitro* autoradiography of the postmortem human brain.[10] Therefore, we consider that the injected dose used was suitable for studying the receptor-radioligand binding and was not a cause of the rapid clearance of [^{11}C]MPDX from the brain.

Because of the rapid clearance of [^{11}C]MPDX from the brain, the distribution of [^{11}C]MPDX might be partially affected by the cerebral blood flow. However, PET images (Fig. 1) showed that the relative uptake levels of [^{11}C]MPDX and [^{15}O]water were different in the striatum, thalamus and cerebellum. When the DV values of [^{11}C]MPDX and the uptake of [^{15}O]water or [^{18}F]FDG were normalized against those in the cerebellum to clarify

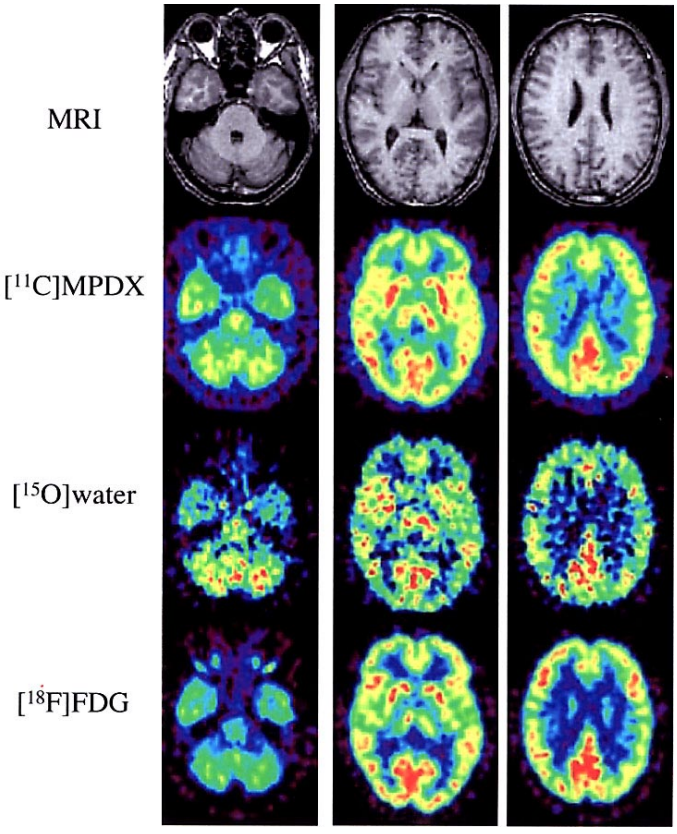

Fig. 1 MRI of the brain and PET images of [^{11}C]MPDX, [^{15}O]water, and [^{18}F]FDG. Top, MRI; second, [^{11}C]MPDX; third, [^{15}O]water; and bottom, [^{18}F]FDG. The static PET images were acquired from 2 to 20 min for [^{11}C]MPDX, from 0 to 2 min for [^{15}O]water, and from 45 to 51 min for [^{18}F]FDG after the injection, and expressed as a relative uptake.

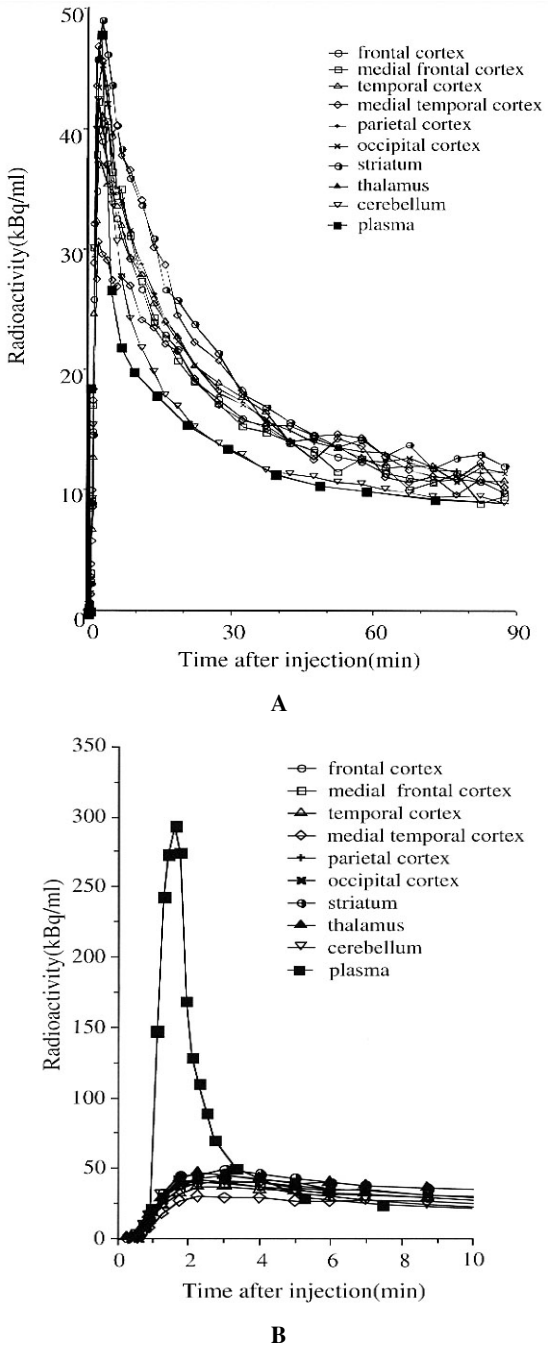

Fig. 2 Time-activity curves in the brain tissues and in plasma after injection of [^{11}C]MPDX. A: Time-activity curves in a 90-min period during PET scan; and B: those in a first 10 min period after injection.

the relationship between the distribution of [^{11}C]MPDX and the cerebral blood flow, the distribution pattern of [^{11}C]MPDX was clearly different from those of [^{15}O]water and [^{18}F]FDG (Fig. 3). The regional brain images and distribution patterns of both blood flow and [^{18}F]FDG were compatible with the database of normal resting subjects in the resting states in our laboratory. The statistical evaluation for the relationship between the distribution of [^{11}C]MPDX and cerebral blood flow is difficult in the present first trial of [^{11}C]MPDX PET in man, but is under investigation.

In the literatures the adenosine A_1 receptors are rich in the hippocampus, cerebral cortex, thalamic nuclei, basal ganglia and the cerebellar cortex in animals[11–13] and humans.[10,14] In the present PET study, the binding of [^{11}C]MPDX evaluated quantitatively as the DV was relatively higher in the striatum and thalamus among the brain regions investigated. The distribution pattern of [^{11}C]MPDX was consistent with the receptor distribution pattern *in vitro* in previous reports,[10–14] except that the DV of [^{11}C]MPDX was relatively smaller in the medial temporal lobe including the hippocampus and cerebellum (Fig. 3). In *in vitro* autoradiography of postmortem human brain, Svenningsson et al. demonstrated that the density of adenosine A_1 receptor binding sites of [^{3}H]8-cyclopentyl-1,3-dipropylxanthine was high in the stratum radiatum/pyramidale of CA1 in the hippocampus but relatively low in other areas in the hippocampus, and was high in the cortex molecular/Purkinje layer while low in the cortex

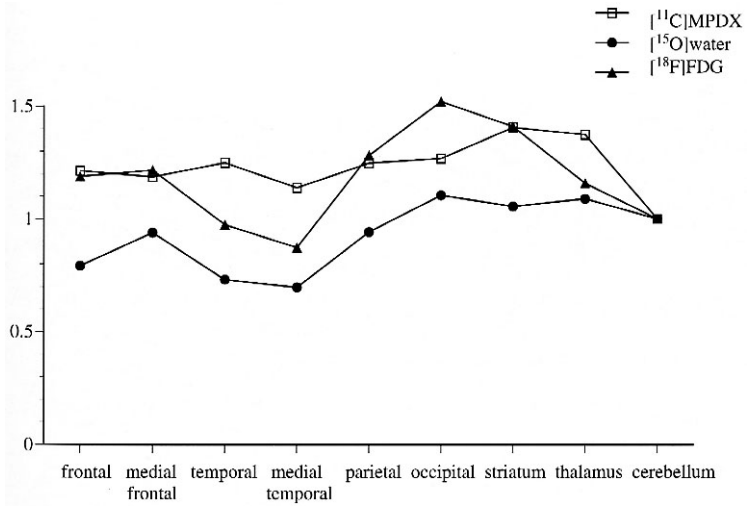

Fig. 3
Relative distribution of [^{11}C]MPDX, [^{15}O]water, and [^{18}F]FDG in the human brain. The distribution volume for [^{11}C]MPDX was measured in each region. Uptake in each region was measured as mean values acquired from 0 to 2 min for [^{15}O]water, and from 45 to 51 min for [^{18}F]FDG. The distribution volume and uptake values were normalized as those for the cerebellum.

granular layer in the cerebellum.[10] In [^{11}C]MPDX PET, the DV values in these ROIs were assessed as the means of high and low densities of the binding sites, which resulted in the apparent discrepancy between the *in vitro* findings and the [^{11}C]MPDX PET in the hippocampus and cerebellum. The partial volume effect based on the spatial resolution may be considered especially in the hippocampus in the PET study.

The adenosine A_1 receptors are distributed both pre- and post-synaptically in all regions of the brain without any reference regions being devoid of them. However, the distribution pattern of [^{11}C]MPDX was different from those of [^{15}O]water and [^{18}F]FDG (Figs. 1 and 3). This finding suggests that the [^{11}C]MPDX PET provides a new diagnostic tool which is distinguished from those based on cerebral blood flow and glucose metabolism. The studies on the postmortem human brain reported a reduced density of adenosine A_1 receptors in the hippocampus of patients with Alzheimer's disease,[15,16] and a significant increase in adenosine A_1 receptor binding in the neocortex obtained from patients suffering from temporal lobe epilepsy.[17] [^{11}C]MPDX PET is of interest in diagnosing patients with neurological and psychiatric diseases, and is under investigation for the progress for diagnosis of the patients with Alzheimer's disease and epilepsy.

In conclusion, [^{11}C]MPDX was widely but discretely distributed with different concentrations in the brain. The graphical analysis showed that the binding of [^{11}C]MPDX was high in the striatum, thalamus, and low in the medial temporal cortex and cerebellum. The distribution pattern of [^{11}C]MPDX was consistent with that of adenosine A_1 receptors *in vitro*. [^{11}C]MPDX PET has the possibility for mapping adenosine A_1 receptors in the human brain.

REFERENCES

1. Collis MG, Hourani SMO. Adenosine receptor subtypes. *Trends Pharmacol Sci* 1993; 14: 360–366.
2. Suzuki F, Ishiwata K. Selective adenosine antagonists for mapping central nervous system adenosine receptors with positron emission tomography: Carbon-11 labeled KF15372 (A_1) and KF17837 (A_{2A}). *Drug Develop Res* 1998; 45: 312–323.
3. Ishiwata K, Shimada J, Ishii K, Suzuki F. Assessment of the adenosine A_{2A} receptors with PET as a new diagnostic tool for neurological disorders. *Drugs Fut* 2002; 27: 569–576.
4. Noguchi J, Ishiwata K, Furuta R, Shimada J, Kiyosawa M, Ishii S, et al. Evaluation of carbon-11 labeled KF15372 and it's ethyl and methyl derivatives as a potential CNS adenosine A_1 receptor ligand. *Nucl Med Biol* 1997; 24: 53–59.
5. Shimada Y, Ishiwata K, Kiyosawa M, Nariai T, Oda K, Toyama H, et al. Mapping adenosine A_1 receptors in the cat brain by positron emission tomography with [^{11}C]MPDX. *Nucl Med Biol* 2002; 29: 29–37.
6. Ishiwata K, Nariai T, Kimura Y, Oda K, Kawamura K, Ishii K, et al. Preclinical studies on [^{11}C]MPDX for mapping adenosine A_1 receptors by positron emission tomography. *Ann Nucl Med* 2002; 16: 377–382.
7. Wang WF, Ishiwata K, Kiyosawa M, Shimada J, Senda M, Mochizuki M. Adenosine A_1 and benzodiazepine receptors and glucose metabolism in the visual structures of rats monocularly deprived by enucleation or eyelid suture at a sensitive period. *Jpn J Ophthal* 2003; 47: 182–190.
8. Ardekani BA, Braun M, Hutton BF, Kanno I, Iida H. A fully automatic multimodality image registration algorithm. *J Comput Assist Tomogr* 1995; 19: 615–623.
9. Logan J, Fowler JS, Volkow ND, Wolf AP, Dewey SL, Schlyer DJ, et al. Graphical analysis of reversible radioligand binding from time-activity measurements applied to [*N*-^{11}C-methyl]-(−)-cocaine PET studies in human subjects. *J Cereb Blood Flow Metab* 1990; 10: 740–747.
10. Svenningsson P, Hall H, Sedvall G, Fredholm BB. Distribution of adenosine receptors in the postmortem human brain: an extended autoradiographic study. *Synapse* 1997; 27: 322–335.
11. Lewis ME, Patel J, Moon Edley S, Marangos PJ. Autoradiographic visualization of rat brain adenosine receptors using N^6-cyclohexyl[^{3}H]adenosine. *Eur J Pharmacol* 1981;

73: 109–110.
12. Goodman RR, Snyder SH. Autoradiographic localization of adenosine receptors in rat brain using [^{3}H]cyclohexyladenosine. *J Neurosci* 1982; 2: 1230–1241.
13. Fastbom J, Pazos A, Palacios JM. The distribution of adenosine A1 receptors and 5′-nucleotidase in the brain of some commonly used experimental animals. *Neuroscience* 1987; 22: 813–826.
14. Fastbom J, Pazos A, Probst A, Palacios JM. Adenosine A1 receptors in the human brain: a quantitative autoradiographic study. *Neuroscience* 1987; 22: 827–839.
15. Jansen K, Faull RLM, Dragunow M, Synek BJL. Alzheimer's disease: changes in hippocampal *N*-methyl-D-aspartate, quisqualate, neurotensin, adenosine, benzodiazepine, serotonin and opioid receptors—an autoradiographic study. *Neuroscience* 1990; 39: 613–627.
16. Ulas J, Brunner LC, Nguyen L, Cotman CW. Reduced density of adenosine A1 receptors and preserved coupling of adenosine A1 receptors to G proteins in Alzheimer hippocampus: a quantitative autoradiographic study. *Neuroscience* 1993; 52: 843–854.
17. Angelatou F, Pagonopoulou O, Maraziotis T, Olivier A, Villemeure JG, Avoli M, et al. Upregulation of A1 adenosine receptors in human temporal lobe epilepsy: a quantitative autoradiographic study. *Neurosci Lett* 1993; 163: 11–14.